

Fluorescence Quenching of Alpha-Fetoprotein by Gold Nanoparticles: Effect of Dielectric Shell on Non-Radiative Decay

Jian Zhu · Jian-jun Li · A-qing Wang ·
Yu Chen · Jun-wu Zhao

Received: 13 April 2010 / Accepted: 7 June 2010 / Published online: 15 June 2010
© The Author(s) 2010. This article is published with open access at Springerlink.com

Abstract Fluorescence quenching spectrometry was applied to study the interactions between gold colloidal nanoparticles and alpha-fetoprotein (AFP). Experimental results show that the gold nanoparticles can quench the fluorescence emission of adsorbed AFP effectively. Furthermore, the intensity of fluorescence emission peak decreases monotonously with the increasing gold nanoparticles content. A mechanism based on surface plasmon resonance–induced non-radiative decay was investigated to illuminate the effect of a dielectric shell on the fluorescence quenching ability of gold nanoparticles. The calculation results show that the increasing dielectric shell thickness may improve the monochromaticity of fluorescence quenching. However, high energy transfer efficiency can be obtained within a wide wavelength band by coating a thinner dielectric shell.

Keywords Fluorescence quenching · Gold nanoparticles · Alpha-fetoprotein (AFP) · Non-radiative decay · Dielectric shell

Introduction

Noble metal colloids, such as gold and silver nanoparticles, allow effective fluorescence quenching over a broad range of wavelengths, which is to be used across a vast spectrum of applications such as energy transfer assays for the detection of proteins [1–4]. As we know, sensitive

analytical technology for quantification of protein concentration in solution is important in biological science [5]. The application of fluorescence quenching is a powerful technique for protein measurement and analysis [6, 7]. Comparing with other commonly used methods to determine protein concentration, the method based on fluorescence resonance energy transfer has a greatly improved sensitivity [3]. For example, Pihlasalo et al. [3] reported a new and highly sensitive method to detect protein concentrations relying on protein adsorption on gold colloids and quenching of fluorescently labeled protein. This assay allowed the determination of picogram quantities of proteins with an average variation of 4.5% in a 10-min assay. Mayilo et al. [8] report the homogeneous sandwich immunoassay with gold nanoparticles (AuNPs) as fluorescence quenchers. A limit of detection of 0.7 ng/ml was obtained for protein cardiac troponin T (cTnT), which is the lowest value reported for a homogeneous sandwich assay for cTnT. Guan et al. [9] utilize the “superquenching” property of AuNPs to polythiophene derivatives for detecting aspartic acid (Asp) and glutamic acid (Glu) in pure water. A sensitive method for detecting Asp and Glu is established with 32 nM and 57 nM as limit of detection for Asp and Glu, respectively.

A resonance energy transfer model based on non-radiative decay provides a theoretical understanding of these observations of fluorescence quenching. The optical properties of molecules adsorbed on or enclosed in metallic and dielectric particles have been investigated both experimentally and theoretically in recent years [10–13]. When a particle has been excited and is oscillating in the incident electromagnetic field, the excited system may have a fluctuating electric dipole moment and causes the radiation [10]. This light radiation from dipole moment provides the channel for radiative decay. On the other hand, the Joule

J. Zhu · J. Li · A.-q. Wang · Y. Chen · J. Zhao (✉)
The Key Laboratory of Biomedical Information Engineering
of Ministry of Education, School of Life Science
and Technology, Xi'an Jiaotong University, Xian Ning West
Road 28#, 710049 Xi'an, People's Republic of China
e-mail: nanoptzhao@163.com

heating and plasmon absorption caused by these fields open the non-radiative decay channels [14, 15]. The competition between radiative decay and non-radiative decay energy transfer affects the fluorescence emission of the molecules located near the particle. If the non-radiative takes the dominating effect, fluorescence quenching occurs. The different distance behavior of the radiative and non-radiative rates explains why the apparent quantum yield always vanishes at short distance from a metallic nanoparticle [11].

Alpha-fetoprotein (AFP) is an oncofetal protein, which has been widely used as a tumor marker for diagnosis and management of hepatocellular carcinoma [16–18]. Many efforts such as amperometric immunosensor [19], enhanced chemiluminescent (CL) immunoassay [16] and fluoroimmunoassay [2] have been developed to improve the sensitivity on detecting AFP level in human serum. Although the fluorescence spectral properties of AFP have already been studied [20], the effect of gold nanoparticles on the fluorescence emission of AFP has seldom been reported. Especially, when protein molecules such as AFP are adsorbed on the gold particle, there will be a dielectric shell. How does the dielectric shell affect the non-radiative energy transfer and fluorescence quenching is also an interesting topic. In this paper, we studied the effect of gold colloids with different concentration on the fluorescence quenching of AFP. By calculating the quantum efficiency as a function of shell thickness, we discuss in detail the quenching mechanism based on SPR-induced non-radiative decay of the dielectric shell-coated gold nanospheres.

Experimental

Gold colloid nanoparticles with spherical shape were synthesized by sodium citrate reduction of HAuCl_4 as reported earlier [9, 21]. The AFP standard samples were obtained from Biocell Biotechnology Co. Ltd (China). The solutions of AFP were prepared in ultra-pure water at room temperature by directly dissolved to prepare stock solutions of 3, 6, 9, and 40 ng/ml, respectively. When the comparison of fluorescence spectra between pure AFP (6 ng/ml) and solution containing both AFP and gold colloid was studied, the solution containing both AFP and gold colloid was obtained by mixing 1 ml gold colloid with 2 ml pure AFP solution (9 ng/ml). So AFP concentration was kept fixed at 6 ng/ml for all samples. When the fluorescence spectra of solution containing both AFP and gold colloid with different gold particle content were studied, the high AuNPs concentration sample was obtained by mixing 2 ml pure AFP (40 ng/ml) with 1.5 ml gold colloid and 0.5 ml ultra-pure water; the medium AuNPs concentration sample was obtained by mixing 2 ml pure AFP (40 ng/ml) with 1.0 ml gold colloid and 1.0 ml ultra-pure water; the low AuNPs

concentration sample was obtained by mixing 2 ml pure AFP (40 ng/ml) with 0.5 ml gold colloid and 1.5 ml ultra-pure water. Fluorescence emission and excitation spectra were carried out on a Perkin–Elmer LS 55 spectrofluorometer. The fluorescence excitation spectra were registered in the range from 250 to 320 nm. The fluorescence emission spectra were registered in the range from 250 to 500 nm.

Results and Discussion

The fluorescence excitation spectrum of pure AFP with a concentration of 3 ng/ml in Fig. 1 is the scanning excited wavelength from 200 to 320 nm when the detection wavelength was located at 345 nm (the fluorescence emission peak of AFP usually takes place at the wavelength range from 320 to 350 nm [20]). The experimental result in Fig. 1 shows that there is a broad exciting band with two peaks at around 260 and 293 nm, respectively, which indicates that the fluorescence emission of AFP at 345 nm is sensitive to the excitation from 260 to 293 nm.

The fluorescence emission spectrum of pure AFP with a concentration of 6 ng/ml in Fig. 2 is the scanning detection wavelength from 250 to 500 nm when the exciting wavelength was located at 293 nm. It is obvious that there is a strong fluorescence emission peak noted at 345 nm. However, when amount of gold colloids were dropped into the AFP solution (the concentration of AFP is kept at 6 ng/ml), the emission peak at 345 nm decreases distinctly, as shown in Fig. 2. This experimental result indicates that the gold nanoparticles can quench the fluorescence of AFP. Fluorescence emission spectra of solution containing both AFP and gold colloid with different gold particle content are compared in Fig. 3. In this comparison, all the samples have the same AFP concentration and the exciting wavelength was located at 260 nm. It is interesting to note that the

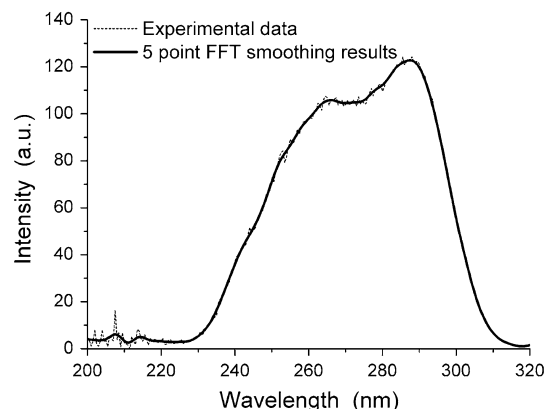


Fig. 1 Fluorescence excitation spectrum of pure AFP solution with a concentration of 3 ng/ml, detection wavelength is 345 nm

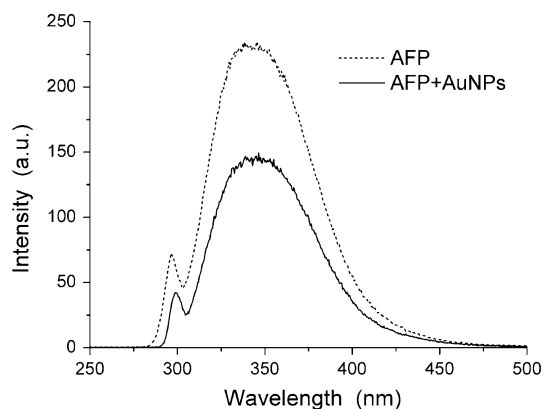


Fig. 2 Comparison of fluorescence emission spectra between pure AFP and solution containing both AFP and gold colloid, exciting wavelength is 293 nm

increasing gold colloid content leads to a decrease in the fluorescence emission peak, as shown in Fig. 3.

The observed fluorescence quenching is attributed to the resonance energy transfer from AFP to gold nanoparticles. This non-radiative decay can be theoretically studied by using the Förster energy transfer theory [11, 22]. When some amounts of gold colloidal nanoparticles are dropped into the solutions of AFP, AFP molecules would tend to cluster around gold particles due to physical adsorption. Increasing the AFP concentration leads to more and more molecules adsorb on the gold particles, so the gold particle will be coated by a dielectric shell. The thickness and dielectric constant of the shell are controlled by the concentration of AFP and gold colloid content. In order to find the effect of the dielectric shell on the fluorescence quenching from gold particle, we calculated the quantum efficiency of the shell-coated gold nanosphere [11],

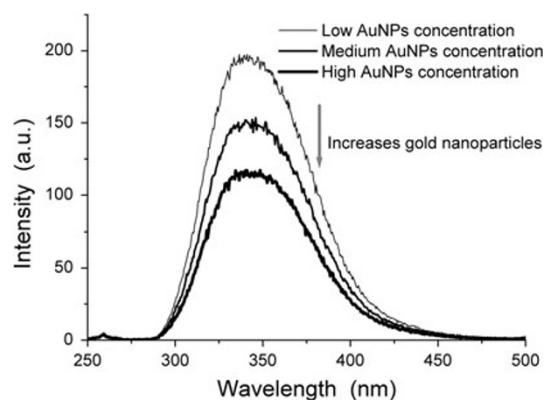


Fig. 3 Fluorescence emission spectra of solution containing both AFP and gold colloid with different gold nanoparticle content, exciting wavelength is 260 nm

The polarizability α of this dielectric shell-coated gold sphere can be obtained from the quasi-static theory [23],

$$\alpha = \frac{4\pi\epsilon_0 r_2^3 [r_2^3(\epsilon_1 + 2\epsilon_2)(\epsilon_2 - \epsilon_3) + r_1^3(\epsilon_1 - \epsilon_2)(2\epsilon_2 + \epsilon_3)]}{2r_1^3(\epsilon_1 - \epsilon_2)(\epsilon_2 - \epsilon_3) + r_2^3(\epsilon_1 + 2\epsilon_2)(\epsilon_2 + 2\epsilon_3)} \tag{2}$$

In this calculation, the gold core has radius $r_1 = 15$ nm and dielectric function ϵ_1 , the dielectric shell has a thickness $r_2 - r_1$ and dielectric constant ϵ_2 (when $\epsilon_2 = 2.0$, the gold particle is coated by a shell; when $\epsilon_2 = \epsilon_3 = 1.0$, no dielectric shell is coated on the gold particle), the embedding medium has dielectric function $\epsilon_3 = 1.0$. In Drude model, this frequency-dependent complex dielectric constant of gold particle can be written as [24]

$$\epsilon_1(\omega) = \epsilon_{1r} + i\epsilon_{1i} = \epsilon_b(\omega) - \frac{\omega_p^2}{\omega^2} + i\frac{\omega_p^2}{\omega\tau(1 + \frac{1}{\omega^2\tau^2})}, \tag{3}$$

$$Q = \frac{\Gamma^R}{\Gamma^R + \Gamma^{NR}} = \frac{1 + \frac{k^6}{4\pi^2}|\alpha|^2[(kz)^{-6} + (kz)^{-4}] + \frac{k^3}{\pi}\text{Re}[\alpha](kz)^{-3}}{1 + \frac{k^6}{4\pi^2}|\alpha|^2[(kz)^{-6} + (kz)^{-4}] + \frac{k^3}{\pi}\text{Re}[\alpha](kz)^{-3} + \frac{3k^3}{2\pi}[\text{Im}[\alpha] - \frac{k^3}{6\pi}|\alpha|^2][(kz)^{-6} + (kz)^{-4}]} \tag{1}$$

In Eq. 1, Γ^R denotes the radiative decay rate, Γ^{NR} denotes the non-radiative decay rate, $k = 2\pi/\lambda$ denotes the wave number of the light, z denotes the distance from particle center to the attached molecule. In our calculation, we study the attached molecule at the outer surface of the shell. So the value of z is equal to the radius of the dielectric shell r_2 , which is changing from 15 to 65 nm.

where $\epsilon_b(\omega)$ is dielectric function of bulk metal which is due to inter-band transition and varies with frequency, these numerical parameters are given in [25]. $\omega_p = 9$ eV denotes the plasmon frequency of the bulk metal [26], τ is the size limit relaxation time of gold nanoparticle [27, 28] and ω is the frequency of electromagnetic wave.

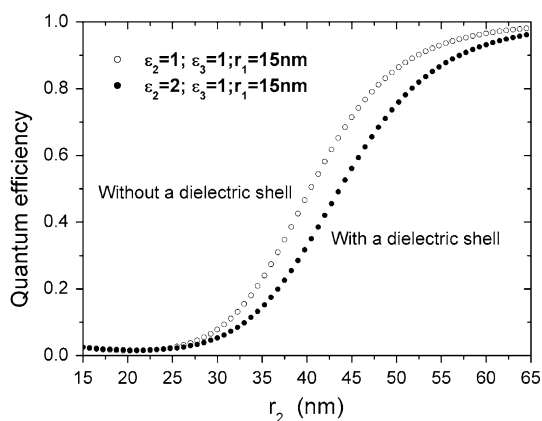


Fig. 4 Quantum efficiency as a function of separation distance at SPR frequency

As shown in Fig. 4, the quantum efficiency at SPR frequency is calculated as a function of separation distance from the particle center to the outer surface of the dielectric shell. Increasing the separation distance leads to a non-linear increase in quantum efficiency. The changing speed is relatively weak at very short and very far distance. These results are similar to the reports of [29]. In order to find the effect of the dielectric shell on this distance-dependent quantum efficiency, the curves corresponding to gold sphere with a dielectric shell and without a shell are compared in Fig. 4. When $\epsilon_2 = \epsilon_3$, the gold sphere is immersed in a dielectric environment and no shell coated on the gold sphere indeed. In this case, r_2 only denotes the distance from particle center to the attached molecule. When $\epsilon_2 \neq \epsilon_3$, the gold sphere is coated with a dielectric shell (the dielectric constant is $\epsilon_2 = 2.0$) first and then immersed in a dielectric environment (the dielectric constant is $\epsilon_3 = 1.0$). The calculated results show that the existence of dielectric shell reduces the quantum efficiency. This reduction begins to take effect when the shell thickness exceeds 10 nm and gets intense with the increasing shell thickness. This reduction of quantum efficiency also indicates the quenching efficiency of a shell-coated gold particle starts to decrease at a farer distance at resonance frequency.

As we know, the fluorescence wavelength is not always matching the SPR frequency of gold nanoparticle. Especially, the fluorescence wavelength of the attached molecule is fixed, whereas the SPR frequency of coated gold nanosphere is tunable by the shell thickness. In order to find the quantum efficiency at different frequency, we plotted the quantum efficiency as a function of wavelength with different shell thickness, as shown in Fig. 5. It is interesting to note that increasing the shell thickness leads to the quantum efficiency peak red shifts, attenuates and narrows down. The shift and narrow down speed is fast with thinner shell and slow with thicker shell. However, the

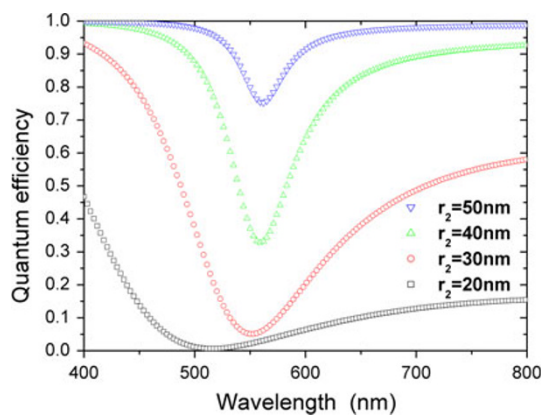


Fig. 5 Quantum efficiency as a function of wavelength with different dielectric shell thickness

attenuate speed is slow with thinner shell and fast with thicker shell. These results show that increasing the dielectric shell thickness may improve the monochromaticity of fluorescence quenching. High energy transfer efficiency can be obtained within a wide wavelength band when coated by a thinner shell. This conclusion is in

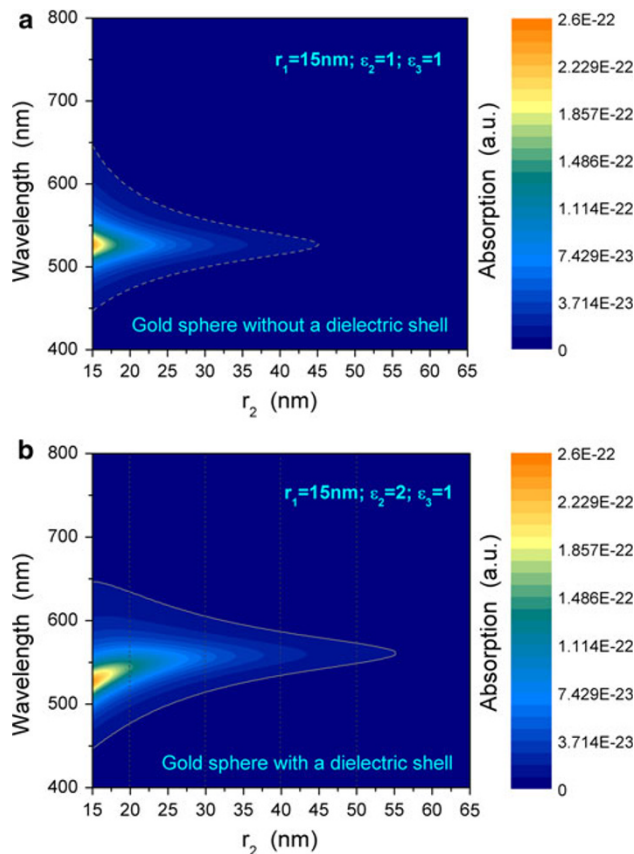


Fig. 6 Absorption cross-section as a function of wavelength and distance from the gold particle center, **a** $\epsilon_2 = \epsilon_3$, **b** $\epsilon_2 > \epsilon_3$

agreement with our experimental results. Increasing the gold particle content leads to a decrease in particle separation and reduces the shell thickness. Therefore, the fluorescence emission decreases with the increasing gold colloids.

Our next goal is to find the physical origin of the quantum efficiency of dielectric shell-coated gold nanoparticle. We believe the SPR absorption is the most important factor that affects the quantum efficiency of a single dipole emitter close to a gold nanoparticle. Therefore, we plotted the absorption cross-section as a function of wavelength and separation distance, as shown in Fig. 6. When $\epsilon_2 = \epsilon_3$, the shell has the same dielectric constant of the embedding medium, thus there is no shell coated on the gold particle indeed. However, in order to make a comparison, we still assumed that there is a shell and calculated absorption cross-section of this dielectric shell-coated gold particle on the condition of $\epsilon_2 = \epsilon_3$, as shown in Fig. 6a. In this case, the absorption intensity decreases rapidly with the increasing separation distance. However, when $\epsilon_2 > \epsilon_3$, the existence of the dielectric shell may slow down the decreasing speed of the absorption cross-section and then reduces the quantum efficiency, as shown in Fig. 6b. Therefore, the existence of dielectric shell may weaken the quantum efficiency of gold nanoparticle, which is in agreement with the results in Fig. 4. Figure 6b also shows that the resonance absorption at SPR frequency is intense with thin dielectric shell and decreases as the shell gets thicker. However, the off-resonance absorption, which is far away from SPR frequency, is very weak and is not sensitive to the shell thickness. Therefore, the changing range of absorption intensity is larger for thinner shell but smaller for thicker shell, which results in the narrow down of the quantum efficiency band with the increasing shell thickness. This conclusion is in agreement with the result in Fig. 5.

Conclusion

Fluorescence quenching of AFP has been observed in the presence of colloidal gold nanoparticles. The quenching effect can be improved by increasing the gold nanoparticle content. Based on non-radiative energy transfer theory, we explained the observed fluorescence quenching characters by calculating the quantum efficiency as a function of dielectric shell thickness. The calculated results show that, because of the SPR-induced non-radiative decay, high energy transfer efficiency and intense fluorescence quenching can be obtained within a wide wavelength band when the gold particles are coated by a thinner dielectric shell.

Acknowledgments This work was supported by the National High-tech Research and Development Program (863 Program) of China under grant No. 2009AA04Z314 and the Fundamental Research Funds for the Central Universities under grant No. xjj20100049.

Open Access This article is distributed under the terms of the Creative Commons Attribution Noncommercial License which permits any noncommercial use, distribution, and reproduction in any medium, provided the original author(s) and source are credited.

References

1. T. Soller, M. Ringler, M. Wunderlich, T.A. Klar, J. Feldmann, H.P. Josel, Y. Markert, A. Nichtl, K. Kürzinger, Radiative and nonradiative rates of phosphors attached to gold nanoparticles. *Nano Lett.* **7**, 1941–1946 (2007)
2. L. Ao, F. Gao, B. Pan, R. He, D. Cui, Fluoroimmunoassay for antigen based on fluorescence quenching signal of gold nanoparticles. *Anal. Chem.* **78**, 1104 (2006)
3. S. Pihlasalo, J. Kirjavainen, P. Hänninen, H. Härmä, Ultrasensitive protein concentration measurement based on particle adsorption and fluorescence quenching. *Anal. Chem.* **81**, 4995–5000 (2009)
4. I. Delfino, S. Cannistraro, Optical investigation of the electron transfer protein azurin-gold nanoparticle system. *Biophys. Chem.* **139**, 1–7 (2009)
5. S. Freddi, L. D'Alfonso, M. Collini, M. Caccia, L. Sironi, G. Tallarida, S. Caprioli, G. Chirico, Excited-state lifetime assay for protein detection on gold colloids-fluorophore complexes. *J. Phys. Chem. C* **113**, 2722–2730 (2009)
6. C.C. Huang, C.K. Chiang, Z.H. Lin, K.H. Lee, H.T. Chang, Bioconjugated gold nanodots and nanoparticles for protein assays based on photoluminescence quenching. *Anal. Chem.* **80**, 1497–1504 (2008)
7. B.N. Giepmans, S.R. Adams, M.H. Ellisman, R.Y. Tsien, The fluorescent toolbox for assessing protein location and function. *Science* **312**, 217–224 (2006)
8. S. Mayilo, M.A. Kloster, M. Wunderlich, A. Lutich, T.A. Klar, A. Nichtl, K. Kürzinger, F.D. Stefani, J. Feldmann, Long-range fluorescence quenching by gold nanoparticles in a sandwich immunoassay for cardiac Troponin T. *Nano Lett.* **9**, 4558–4563 (2009)
9. H.L. Guan, P. Zhou, X.L. Zhou, Z.K. He, Sensitive and selective detection of aspartic acid and glutamic acid based on polythiophene-gold nanoparticles composite. *Talanta* **77**, 319–324 (2008)
10. J. Gersten, A. Nitzan, Spectroscopic properties of molecules interacting with small dielectric particles. *J. Chem. Phys.* **75**, 1139–1152 (1981)
11. R. Carminati, J.J. Greffet, C. Henkel, J.M. Vigoureux, Radiative and non-radiative decay of a single molecule close to a metallic nanoparticle. *Opt. Commun.* **261**, 368–375 (2006)
12. J. Zhu, Enhanced fluorescence from Dy^{3+} owing to surface plasmon resonance of Au colloid nanoparticles. *Mater. Lett.* **59**, 1413–1416 (2005)
13. T. Pons, I.L. Medintz, K.E. Sapsford, S. Higashiya, A.F. Grimes, D.S. English, H. Mattoussi, On the quenching of semiconductor quantum dot photoluminescence by proximal gold nanoparticles. *Nano Lett.* **7**, 3157–3164 (2007)
14. E. Dulkeith, A.C. Morteani, T. Niedereichholz, T.A. Klar, J. Feldmann, S.A. Levi, F.C.J.M. van Veggel, D.N. Reinhoudt, M. Moller, D.I. Gittins, Fluorescence quenching of dye molecules near gold nanoparticles: radiative and nonradiative effects. *Phys. Rev. Lett.* **89**, 203002 (2002)

15. Y. Chen, K. Munechika, D.S. Ginger, Dependence of fluorescence intensity on the spectral overlap between fluorophores and plasmon resonant single silver nanoparticles. *Nano Lett.* **7**, 690–696 (2007)
16. X.Y. Yang, Y.S. Guo, S. Bi, S.S. Zhang, Ultrasensitive enhanced chemiluminescence enzyme immunoassay for the determination of α -fetoprotein amplified by double-codified gold nanoparticles labels. *Biosens. Bioelectron.* **24**, 2707–2711 (2009)
17. W.C. Tsai, I.C. Lin, Development of a piezoelectric immunosensor for the detection of alpha-fetoprotein. *Sens. Actuator B Chem.* **106**, 455–460 (2005)
18. Y.F. Chang, R.C. Chen, Y.J. Lee, S.C. Chao, L.C. Su, Y.C. Li, C. Chou, Localized surface plasmon coupled fluorescence fiber-optic biosensor for alpha-fetoprotein detection in human serum. *Biosens. Bioelectron.* **24**, 1610–1614 (2009)
19. Y.Y. Xu, C. Bian, S. Chen, S. Xia, A microelectronic technology based amperometric immunosensor for α -fetoprotein using mixed self-assembled monolayers and gold nanoparticles. *Anal. Chim. Acta* **561**, 48–54 (2006)
20. S.S.J. Leong, A.P.J. Middelberg, Dilution versus dialysis: a quantitative study of the oxidative refolding of recombinant human alpha-fetoprotein. *Food Bioprod. Process.* **84**, 9–17 (2006)
21. K.C. Grabar, R.G. Freeman, M.B. Hommer, M.J. Natan, Preparation and characterization of Au colloid monolayers. *Anal. Chem.* **67**, 735–743 (1995)
22. T. Förster, Zwischenmolekulare Energiewanderung und Fluoreszenz. *Ann. Physik.* **2**, 55–75 (1948)
23. R.D. Averitt, S.L. Westcott, N.J. Halas, Linear optical properties of gold nanoshells. *J. Opt. Soc. Am. B* **16**, 1824–1832 (1999)
24. J.A.A.J. Perenboom, P. Wyder, F. Meier, Electronic properties of small metallic particles. *Phys. Rep.* **78**, 173 (1981)
25. P.B. Johnson, R.W. Christy, Optical constants of the noble metals. *Phys. Rev. B* **6**, 4370–4379 (1972)
26. V.I. Belotelova, G. Carotenuto, L. Nicolais, A. Longo, G.P. Pepe, P. Perlo, A.K. Zvezdin, Online monitoring of alloyed bimetallic nanoparticle formation by optical spectroscopy. *J. Appl. Phys.* **99**, 044304 (2006)
27. D. Canchal-Arias, P. Dawson, Measurement and interpretation of the mid-infrared properties of single crystal and polycrystalline gold. *Surf. Sci.* **577**, 95–111 (2005)
28. J. Zhu, Y.C. Wang, L.Q. Huang, Y.M. Lu, Resonance light scattering characters of core-shell structure of Au–Ag nanoparticles. *Phys. Lett. A* **323**, 455–459 (2004)
29. Z. Gueroui, A. Libchaber, Single-molecule measurements of gold-quenched quantum dots. *Phys. Rev. Lett.* **93**, 166108 (2004)